

AN INVESTIGATION OF THE EFFECT OF AN AXIAL
COMPRESSIVE LOAD ON THE NATURAL
FREQUENCY OF A COLUMN

By

Hubert L. Greene

A THESIS

Submitted in partial fulfillment of the requirements
for the degree of Master of Science in the College
of Engineering in the University of Alabama

University, Alabama

1951

74
177

ACKNOWLEDGMENTS

The author is indebted to Professor F. R. Steinbacher, Head of the Aeronautical Engineering Department of the University of Alabama, for his interest, advice and direction in the preparation of this thesis. The author also wishes to thank Professor Harry Majors, Jr., and Professor Warren G. Keith for their many kind and helpful suggestions and their moral support.

To Mr. M. M. McElhiney and Mr. Charles Adams, University mechanics, the author wishes to express his appreciation for their assistance in constructing the testing apparatus and preparing the test specimens.

T378
G-832i
1951

CONTENTS

Chapter		Page
I	INTRODUCTION.	1
II	THEORETICAL DEVELOPMENT	3
III	EXPERIMENTAL TESTING.	17
IV	EXPERIMENTAL RESULTS.	28
V	CONCLUSION.	34
Appendix A.	Damping: Types Present and Effects.	38
Appendix B.	A Resume' of Investigations of Vibration in Aircraft.	42
	BIBLIOGRAPHY.	49

TABLES

Number		Page
1	Theoretical Values for f_n Versus P/P_E for Various L/ρ	14
2	Experimental Values of f_n/f_{n_0} , P/P_E . . .	29
3	Theoretical Values of f_n Versus Load Compared to Experimental Values of f_n Versus Load.	31

FIGURES

Number		Page
1	Theoretical Curves of f_n vs P/P_E for Various Values of L/ρ	15
2	Theoretical Variation of f_n/f_{n_0} with P/P_E for any Long Column.	16
3	Schematic Diagram of Pressure System.	19
4	Schematic Diagram of Vibration Recording System.	20
5	Testing Rig as Seen From Rear	21
6	View of Test Equipment.	22
7	View of Ram End of Specimen Supports.	23
8	Mechanical Oscillator.	24
9	Lissajous Patterns Showing the Ratios of the Frequencies Applied to the Y Axis to Those Applied to the X Axis and with a 90° Phase Difference.	26
10	Theoretical and Experimental Values of f_n/f_{n_0} vs P/P_E	30

NOMENCLATURE

<u>Symbol</u>	<u>Description</u>	<u>Units</u>
A	Area	in. ²
E	Modulus of elasticity	psi
f_n	Natural frequency	cps
f_{nE}	Natural frequency--experimental	cps
f_{nO}	Natural frequency at zero load	cps
f_{nT}	Natural frequency--theoretical	cps
g	Gravitational constant	in./sec ²
I	Moment of inertia	in. ⁴
L	Length	in.
M	Bending moment	
n	Mode of vibration	
P	Load	lb
P_E	Euler critical column load	lb
Q	Shear	
T	Kinetic energy	
V	Potential energy	
γ	Weight of material per unit volume	lb/in. ³
ρ	Radius of gyration	

CHAPTER I

INTRODUCTION

Vibration analysis in recent years has assumed an increasingly important role in engineering progress. In particular, the development of the airplane to its present status has brought forth vibration problems seldom encountered in other fields.

The origin of vibration in an aircraft structure can be considered as arising from two basic sources: namely, aerodynamic and mechanical. In all types of aircraft, vibrations of aerodynamic origin are most prevalent. These vibrations are caused by such aerodynamic forces as fluctuating airloads, gusts, and in some cases compressibility. The vibrations of a mechanical origin are mainly caused by reciprocating engines and propellers.

The aircraft structure as a whole and its components have both mass and elasticity and thereby have the property of freely vibrating at a frequency inherent in all elastic systems. This frequency is called the natural frequency.

The natural frequency of the elastic system has a tendency to change when the mass is changed or the system is under load, or if viscous damping is present.

Vibration caused by external forces is called forced vibration which has the frequency of the exciting force and is independent of the natural frequency of the system. However, when the frequency of the forced vibration coincides with the natural frequency of the system, a resonant condition is encountered and excessive amplitudes may result.¹ Therefore, the determination of the natural frequency of a structural member, in this instance a column, subjected to a change in mass or to loads is of importance.

The purpose of this thesis is to investigate the effect of an axial compressive load on the natural frequency of aluminum and brass columns of circular and tubular cross section, and to check existing theories concerning such changes in natural frequency.

1. For further discussion of resonance see any standard text on vibration.

CHAPTER II

THEORETICAL DEVELOPMENT¹

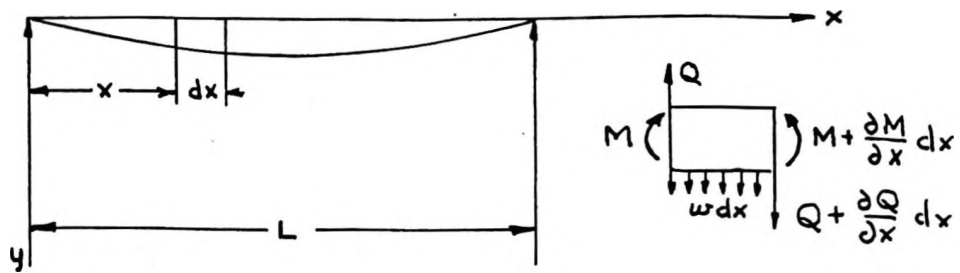


Fig. A

Assuming that vibration occurs in one of the principal planes of flexure of a bar and that the cross sectional dimensions are small in comparison with the length of the bar and is of a homogeneous material, the well-known differential equation of the deflection curve

$$EI \frac{d^2y}{dx^2} = -M \quad (1)$$

will be used, in which

EI is the flexural rigidity and,

M is the bending moment at any cross section.

1. S. Timoshenko, Vibration Problems in Engineering (2nd ed.), pp. 331-333, 338-340, 364-366.

The direction of the axes and the positive directions of bending moments and shearing forces are as shown in Fig. A.

Differentiating equation 1 twice we obtain

$$\frac{d}{dx} \left(EI \frac{d^2 y}{dx^2} \right) = - \frac{dM}{dx} = -Q, \quad (a)$$

$$\frac{d^2}{dx^2} \left(EI \frac{d^2 y}{dx^2} \right) = - \frac{dQ}{dx} = w$$

This last equation representing the differential equation of a bar subjected to a continuous load of intensity w can be used also for obtaining the equation of lateral vibration. It is only necessary to apply D'Alembert's principle and to imagine that the vibrating bar is loaded with inertia forces, the intensity of which varies along the length of the bar and is given by

$$- \frac{\gamma A}{g} \frac{\partial^2 y}{\partial t^2} \quad (b)$$

where γ is the weight of the material of the bar per unit volume, and A is the cross sectional area.

Substituting (b) for w in equation (a) the general equation for the lateral vibration of the bar becomes²

2. Note that no damping is taken into consideration.

$$\frac{\partial^2}{\partial x^2} \left(EI \frac{\partial^2 y}{\partial x^2} \right) = - \frac{\gamma A}{g} \frac{\partial^2 y}{\partial t^2} \quad (2)$$

In the particular case of a prismatical bar the flexural rigidity EI remains constant along the length of the bar and we obtain from equation (2)

$$EI \frac{\partial^4 y}{\partial x^4} = - \frac{\gamma A}{g} \frac{\partial^2 y}{\partial t^2}$$

or

$$\frac{\partial^2 y}{\partial t^2} + a^2 \frac{\partial^4 y}{\partial x^4} = 0 \quad (3)$$

in which

$$a^2 = \frac{EIg}{A\gamma} \quad (4)$$

One begins with studying the normal modes of vibration. When a bar performs a normal mode of vibration the deflection at any location varies harmonically with time and can be represented as follows:

$$y = X (A \cos pt + B \sin pt), \quad (c)$$

where X is a function of the coordinate x determining the shape of the normal mode of vibration under consideration. Such functions are called normal functions. Substituting (c) in equation (3) we obtain,

$$\frac{d^4 X}{dx^4} = \frac{p^2}{a^2} X, \quad (5)$$

from which the normal functions for any particular case can be obtained.

By using the notation

$$\frac{p^2}{a^2} = \frac{p^2 A \gamma}{EI g} = k^4 \quad (6)$$

it can be easily verified that $\sin kx$, $\cos kx$, $\sinh kx$ and $\cosh kx$ will be particular solutions of equation (5) and the general solution of this equation will be obtained in the form,

$$X = A \sin kx + B \cos kx + C \sinh kx + D \cosh kx \quad (7)$$

in which A...D are constants which should be determined in every particular case from the conditions at the ends of the bar. For the two ends of a vibrating bar we always will have four end conditions from which the ratios between the arbitrary constants of the general solution (7) and the frequency equation can be obtained. In this manner the modes of natural vibration and their frequencies will be established. By superimposing all possible normal vibrations (c) the general expression for the free lateral vibrations becomes

$$y = \sum_{n=1}^{\infty} X_n (A_n \cos p_n t + B_n \sin p_n t) \quad (8)$$

In considering particular cases of vibration it is useful to present the general solution, equation (7) in the following form

$$X = C_1 (\cos kx + \cosh kx) + C_2 (\cos kx - \cosh kx) \\ + C_3 (\sin kx + \sinh kx) + C_4 (\sin kx - \sinh kx) \quad (9)$$

In the case of hinged ends the end conditions lead to

$$(1) (X)_{x=0} = 0; \quad (2) \left(\frac{d^2 X}{dx^2} \right)_{x=0} = 0; \\ (3) (X)_{x=1} = 0; \quad (4) \left(\frac{d^2 X}{dx^2} \right)_{x=1} = 0. \quad (d)$$

From the first two conditions (d) it can be concluded that the constants C_1 and C_2 in solution (9) should be taken equal to zero. From conditions (3) and (4) we obtain $C_3 = C_4$ and

$$\sin kL = 0 \quad (10)$$

which is the frequency equation for the case under consideration. The consecutive roots of this equation are

$$kL = \pi, 2\pi, 3\pi, \dots \quad (11)$$

The circular frequencies of the consecutive modes of vibration will be obtained from equation (6)

$$p_1 = ak_1^2 = \frac{a\pi^2}{L^2}; \quad p_2 = \frac{4a\pi^2}{L^2}; \quad p_3 = \frac{9a\pi^2}{L^2}; \dots \quad (12)$$

and the frequency f_n of any mode of vibration will be found from the equation

$$f_n = \frac{p_n}{2\pi} = \frac{n^2 a \pi}{2L^2} = \frac{\pi n^2}{2L^2} \sqrt{\frac{EIg}{AV}} \quad (13)$$

The shape of the deflection curve for the various modes of vibration is determined by the normal function (9). It was shown that in the case under consideration, $C_1 = C_2 = 0$ and $C_3 = C_4$, hence the normal function has the form

$$X = D \sin kx. \quad (e)$$

Substituting for k its values, from equation (11), one obtains

$$X_1 = D_1 \sin \frac{\pi x}{L}; \quad X_2 = D_2 \sin \frac{2\pi x}{L};$$

$$X_3 = D_3 \sin \frac{3\pi x}{L}; \dots\dots$$

It is seen that the deflection curve during vibration is a sine curve, the number of half waves in the consecutive modes of vibration being equal to 1, 2, 3..... By superimposing such sinusoidal vibrations any kind of free vibration due to any initial conditions can be represented. Substituting (e) in the general solution (8) one obtains

$$y = \sum_{n=1}^{\infty} \sin \frac{n\pi x}{L} (E_n \cos p_n t + F_n \sin p_n t) \quad (14)$$

The constants E_n , F_n should be determined in every particular case so as to satisfy the initial conditions.

In considering a bar with hinged ends and compressed by two forces P as shown in Fig. B, the general expression

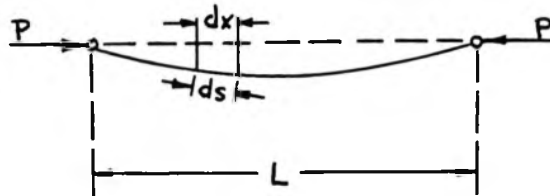


Fig. B

for the lateral vibration will be the same as before (see equation 14).

$$y = \sum_{n=1}^{\infty} q_n \sin \frac{n\pi x}{L} \quad (f)$$

where the symbol q_n denotes the generalized coordinates of equation (14). The difference will be only in the expression for the potential energy of the system. It will be appreciated that during lateral deflection in this case not only the energy of bending but also the change in the energy of compression should be considered. Assuming that the hinges are immovable during vibration, due to

lateral deflection the initially compressed center line of the bar expands somewhat and the potential energy of compression diminishes. The increase in length of the center line will be (see Fig. B),

$$\int_0^L (ds - dx) \approx \frac{1}{2} \int_0^L \left(\frac{dy}{dx} \right)^2 dx$$

Considering only those deflections which are so small that any change in longitudinal force can be neglected, the corresponding diminishing of the energy of compression will be

$$\begin{aligned} \frac{P}{2} \int_0^L \left(\frac{dy}{dx} \right)^2 dx &= \frac{P}{2} \int_0^L \left(\sum_{n=1}^{\infty} q_n \frac{n\pi}{L} \cos \frac{n\pi x}{L} \right)^2 dx \\ &= \frac{P\pi^4}{4L} \sum_{n=1}^{\infty} n^2 q_n^2 \end{aligned} \quad (g)$$

If the ends of the bar are free to slide in an axial direction equation (g) will represent the work done by forces P. For the energy of bending the following equation will be used.

$$\begin{aligned}
V &= \frac{EI}{2} \sum_{n=1}^{\infty} q_n^2 \int_0^L \left(\frac{d^2 X_n}{dx^2} \right)^2 dx \\
&= \frac{EI}{2} \sum_{n=1}^{\infty} q_n^2 \int_0^L \frac{n^4 \pi^4}{L^4} \sin^2 \frac{n\pi x}{L} dx \\
&= \frac{EI\pi^4}{4L^3} \sum_{n=1}^{\infty} n^4 q_n^2
\end{aligned}$$

Hence the complete potential energy becomes

$$V = \frac{EI\pi^4}{4L^3} \sum_{n=1}^{\infty} n^4 q_n^2 - \frac{P\pi^2}{4L} \sum_{n=1}^{\infty} n^2 q_n^2 \quad (15)$$

The kinetic energy of the bar is

$$T = \frac{\gamma AL}{4g} \sum_{n=1}^{\infty} \dot{q}_n^2 \quad (16)$$

and Lagrange's equation for any coordinate q_n will be

$$\frac{\gamma AL}{2g} \ddot{q}_n + \frac{EI\pi^4}{2L^3} \left(n^4 - \frac{PL^2}{EI\pi^2} n^2 \right) q_n = 0$$

By using the notations,

$$\alpha^2 = \frac{EIg}{\gamma A} \quad , \quad \alpha^2 = \frac{PL^2}{EI\pi^2} \quad (17)$$

we obtain

$$\ddot{q}_n + \frac{\alpha^2 \pi^4}{L^4} (n^4 - \alpha^2 n^2) q_n = 0$$

from which

$$q_n = C \cos \left(\frac{\alpha \pi^2 n^2}{L^2} \sqrt{1 - \frac{\alpha^2}{n^2}} \right) t + D \sin \left(\frac{\alpha \pi^2 n^2}{L^2} \sqrt{1 - \frac{\alpha^2}{n^2}} \right) t \quad (18)^3$$

Substituting this in equation (f) the complete expression for free vibrations will be obtained.

Comparing this solution (18) with (12) it can be concluded that, due to the compressive force P , the frequencies of natural vibration are diminished in the proportion

$$\sqrt{1 - \frac{\alpha^2}{n^2}}$$

If α^2 approaches 1, the frequency of the fundamental type of vibration approaches zero, because at this value of α^2 the compressive force P attains its critical value $EI\pi^2/L^2$ at which the straight form of equilibrium becomes unstable and the bar buckles sidewise.

If instead of a compressive a tensile force P is acting on the bar the frequency of vibration increases.

3. This equation was developed for a column, with the following assumptions: A high slenderness ratio, hinged ends, vibration occurring in one of the principal planes of flexure, and with no damping present.

In order to obtain the free vibrations in this case it is only necessary to change the sign of ϵ^2 in equation (18).

Using the equation for the natural frequency of lateral vibration of hinged bars that was presented by Timoshenko, calculations were made for finding the natural frequencies of bars that had different slenderness ratios. The values thus obtained (Table 1) were plotted on a graph whose coordinates were the slenderness ratio and the ratio of P/P_E . In this manner a family of theoretical curves was developed for bars of any material whose slenderness ratios are in the range of 90 to 210. This family of curves is shown on Fig. 1.⁴ When a non-dimensional plot of the ratios f_n/f_{n_0} , where f_{n_0} is the theoretical natural frequency at zero load, and P/P_E was made, it was found that one curve held for all values of L/ρ . The curve was of a parabolic nature and shown on Fig. 2.

4. See p. 3 for the assumptions on which the calculations were based.

TABLE 1

Theoretical Values for f_n Versus P/P_E
for Various L/ρ

$L/\rho =$	93	125	150	160	170	187	210
f_n	P/P_E	P/P_E	P/P_E	P/P_E	P/P_E	P/P_E	P/P_E
0	1.000	1.000	1.000	1.000	1.000	1.000	1.000
5	.999	.998	.997	.997	.996	.996	.994
10	.998	.992	.988	.987	.985	.982	.978
15	.995	.982	.974	.971	.967	.960	.949
20	.988	.968	.954	.948	.941	.923	.910
25	.975	.950	.927	.918	.908	.888	.858
30	.962	.928	.897	.883	.867	.839	.796
35	.948	.903	.860	.842	.819	.782	.723
40	.930	.865	.818	.793	.764	.714	.639
45	.910	.838	.769	.737	.702	.638	.544
50	.891	.801	.714	.676	.632	.554	.435
55	.870	.759	.655	.608	.554	.458	.318
60	.842	.712	.589	.534	.469	.356	.189
65	.815	.663	.518	.452	.378	.242	.046
70	.786	.619	.440	.366	.278	.124	
75	.755	.551	.359	.270	.170		
80	.720	.489	.269	.172	.056		
85	.680	.425	.175	.065			
90	.645	.354	.075				
95	.604	.280					
100	.558	.202					
105	.510	.122					
110	.460	.038					
115	.406						
120	.355						
125	.296						
130	.242						
135	.185						
140	.125						
145	.065						
150	0.000						

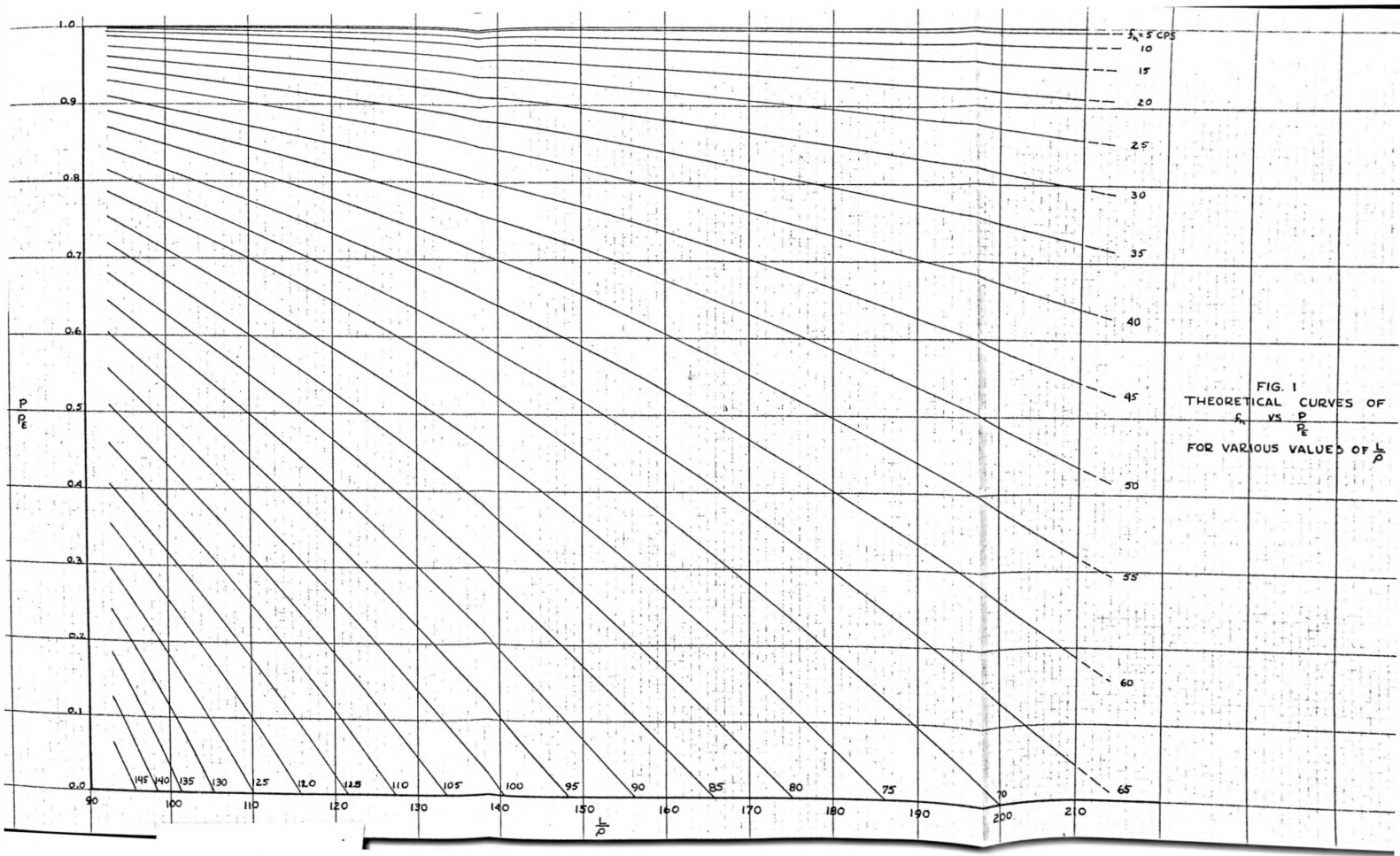


FIG. 1
 THEORETICAL CURVES OF
 f_n VS $\frac{P}{P_E}$
 FOR VARIOUS VALUES OF $\frac{L}{D}$

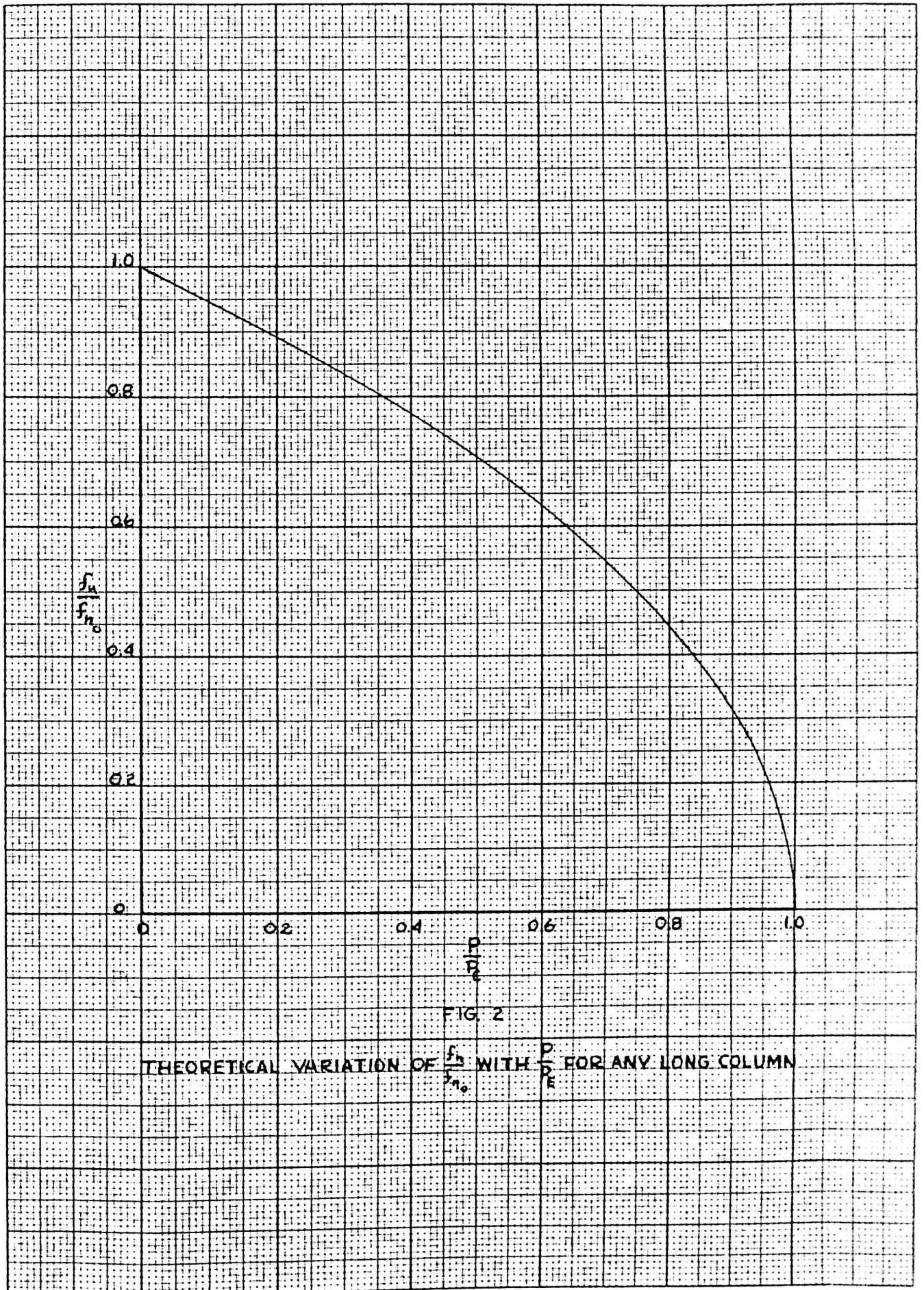


FIG. 2

THEORETICAL VARIATION OF $\frac{f_n}{f_{n_0}}$ WITH $\frac{P}{E}$ FOR ANY LONG COLUMN

CHAPTER III

EXPERIMENTAL TESTING

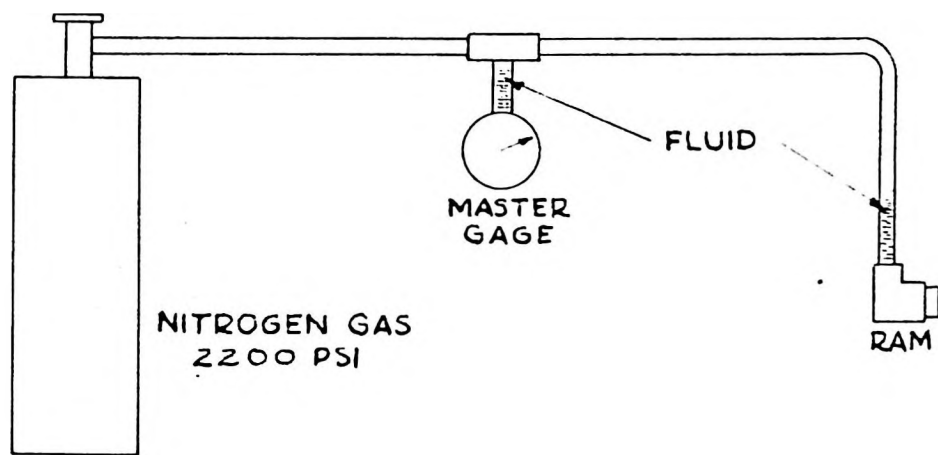
Description of Testing Apparatus

The specimens used were of round 17 ST aluminum alloy rod and seamless brass tubing. Each specimen was 23-3/8 inches long but of a different slenderness ratio. The slenderness ratios were such, however, that the specimens were in the long column range covering a spectrum of L/ρ from 90 to 190. The ends of the aluminum specimens were machined to an angle of 60° and rounded to a radius of 1/4 inch to approximate as closely as possible pinned ends when mounted. Fittings of the same shape were made for the brass tubing.

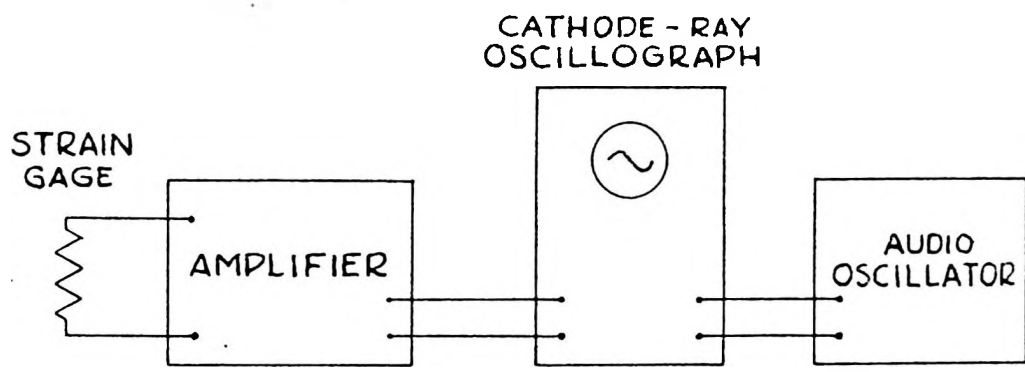
The specimens were mounted in a testing rig which permitted the application of compressive loads to a maximum of 2200 pounds by a ram actuated by a combination of hydraulic fluid and nitrogen gas as shown by a schematic diagram, Fig. 3 and the applied loads were read on a calibrated master fluid gage. The ram was one square inch in area and fitted with a special head that was machined to an angle of 120° and rounded to 1/4 inch radius. The

other end support was of the same shape and was fitted in a stationary holder. The ram support and the stationary end support were rigidly mounted on an eight inch channel and arrangements were made so that a mechanical oscillator could be attached to the channel. The testing rig was suspended from a framework which permitted the rig to vibrate when the oscillator was used.

Bonded wire strain gages of the Baldwin-Southwark SR-4 type A-1 were attached to the center of each specimen. The leads from the strain gages were connected to an amplifier and then to the "y" axis of a DuMont Cathode Ray Oscillograph. An electronic audio oscillator of a frequency range of 20 - 200,000 cps was connected to the "x" axis of the oscillograph. The audio oscillator, calibrated within 2% accuracy was used instead of the uncalibrated linear sweep frequencies of the oscillograph. A schematic diagram of the vibration recording system is shown in Fig. 4.



SCHEMATIC DIAGRAM OF PRESSURE SYSTEM
FIG. 3



SCHEMATIC DIAGRAM OF VIBRATION
RECORDING SYSTEM
FIG. 4

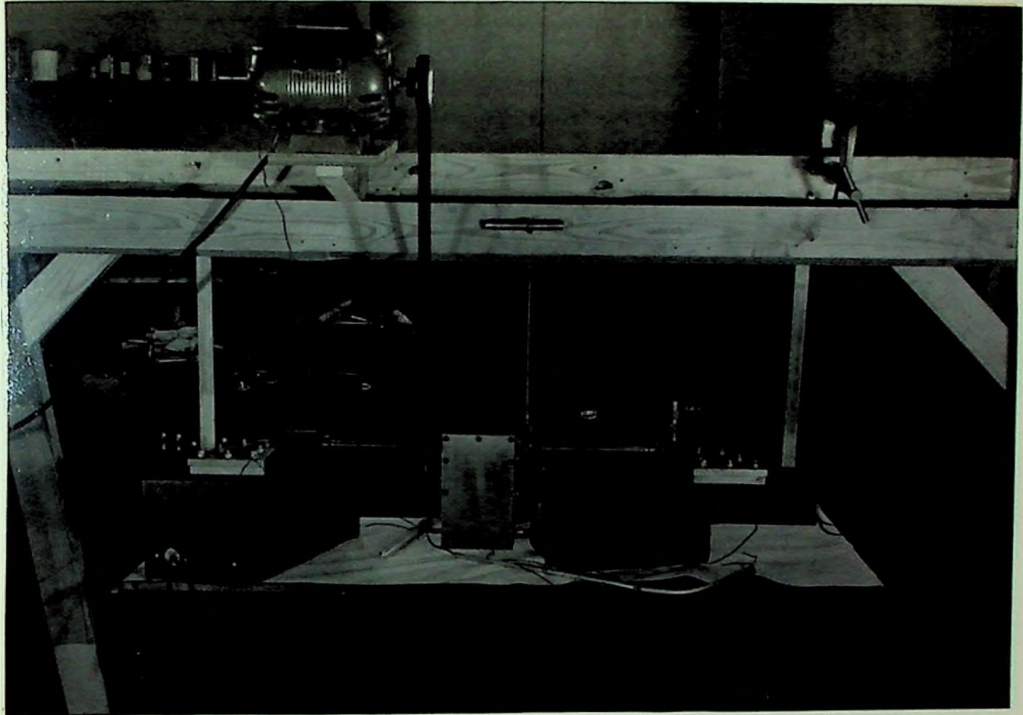


Fig. 5

Testing Rig as Seen From Rear

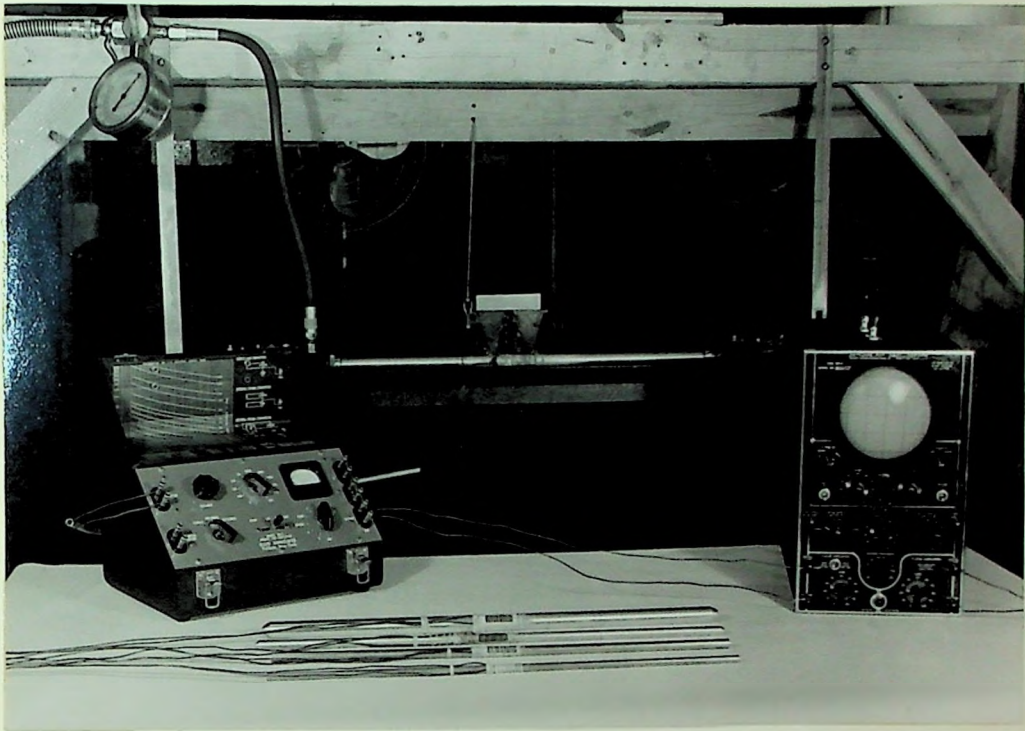


Fig. 6

View of Test Equipment

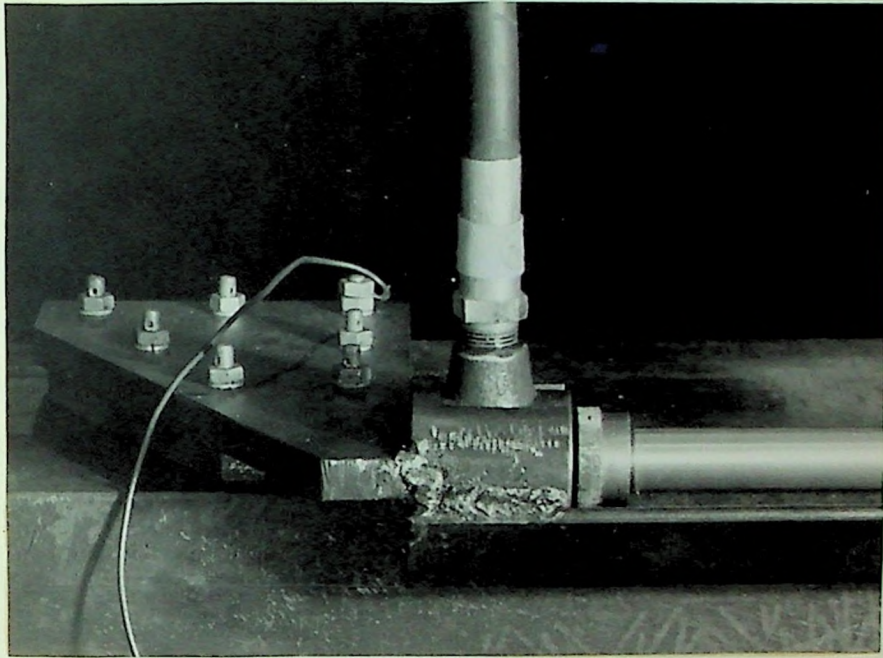


Fig. 7

View of Ram End of Specimen Supports

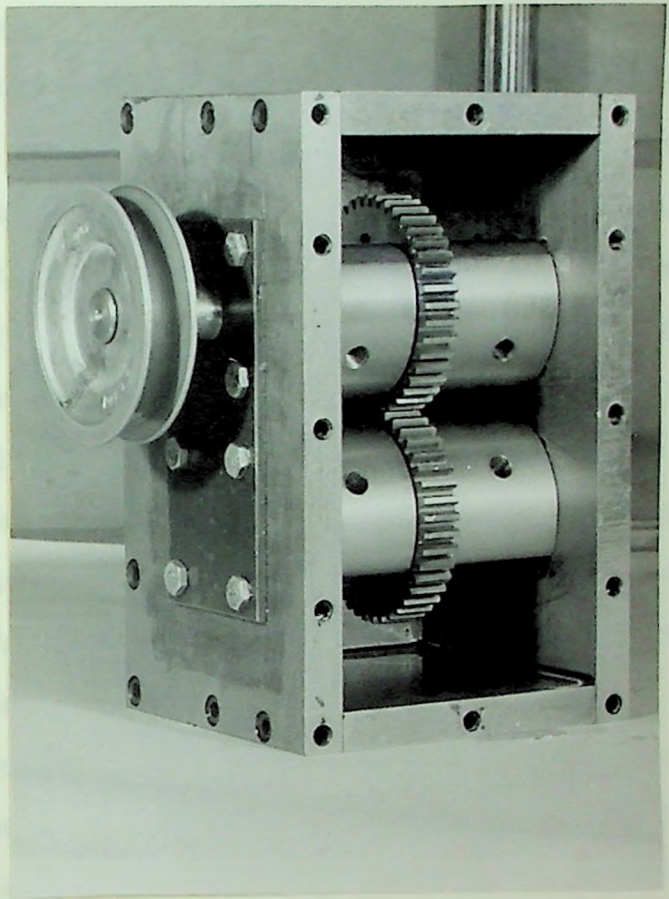


Fig. 8
Mechanical Oscillator

Testing Procedure

The testing procedure consisted of securely mounting the specimen in the test rig, making sure there was no end play of the specimen. The specimen was tapped and the frequency of the free vibration was imposed upon the vertical deflection plates of the cathode ray oscillograph. A frequency from an audio oscillator was imposed upon the horizontal deflection plates of the oscillograph. When the two frequencies were 90° out of phase and of the same value a circle was formed on the screen of the oscillograph as shown in Fig. 9. The value of the free vibration was read on the scale of the audio oscillator. This value of the vibration was then the natural frequency of the specimen in an unloaded condition.

Compressive loads were then applied to the specimen in increments of 100 pounds. At each increment the specimen was tapped near the center of the specimen by a wooden mallet and the frequency was determined in the same manner as in the unloaded condition.

At the higher frequencies of vibration the calibration of the oscillator was such that close values of frequency could not be determined with ease. Therefore, utilizing the method of determining frequencies by Lissajous figures, lower frequencies were introduced from

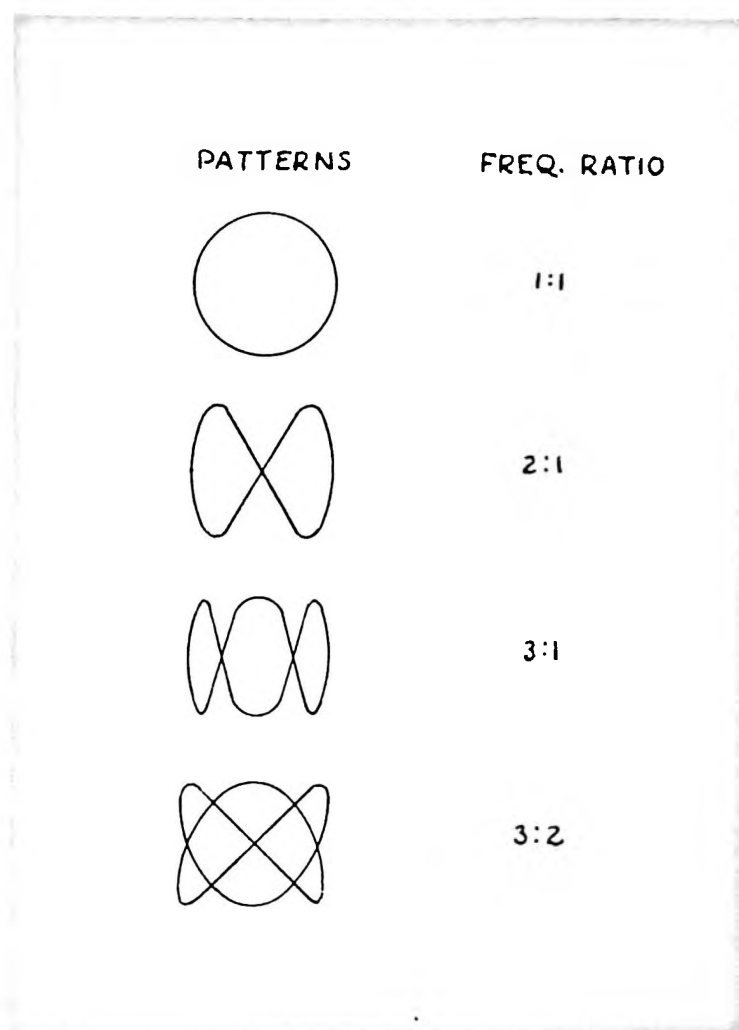


Fig. 9

Lissajous Patterns Showing the Ratios of
the Frequencies Applied to the Y
Axis to Those Applied to the
X Axis and with a 90°
Phase Difference

the oscillator and the frequency of vibration of the specimen was determined by the frequency ratio.

The specimens were loaded to buckling and then unloaded in increments of 100 pounds. At each increment of unloading the frequency of vibration of the specimen was again determined as a check.

In order to determine the action of a loaded specimen when subjected to a forced frequency of vibration, the test rig was vibrated by a mechanical oscillator at a frequency of 66 cycles per second. The specimen was first vibrated at zero load and then at loads in 100 pound increments until the critical load was reached. The amplitude of vibration of the specimen was checked at each increment of the load by a stroboscope.

CHAPTER IV

EXPERIMENTAL RESULTS

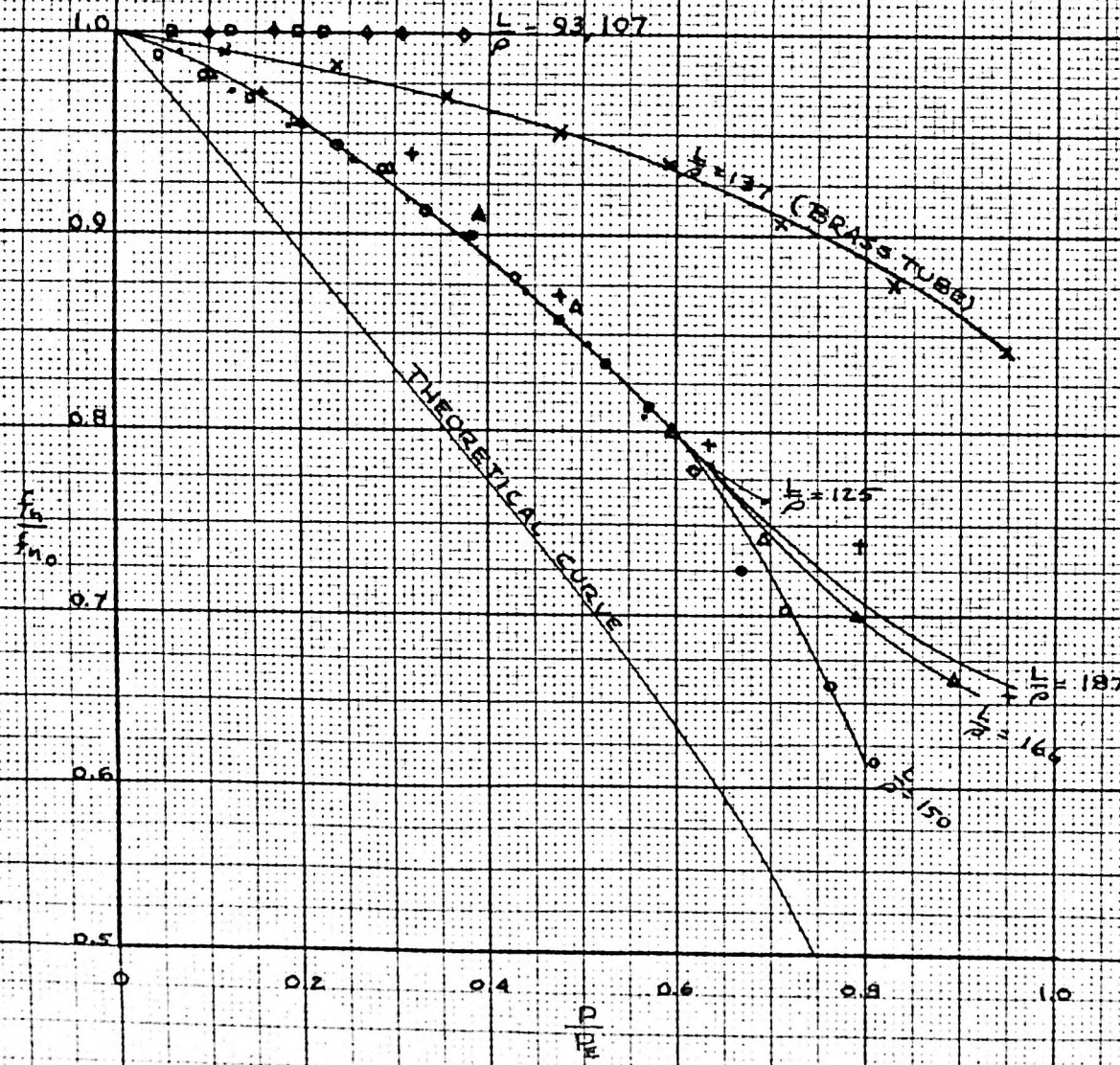
The experimental values of the natural frequencies plotted in the ratio of f_n/f_{n_0} versus P/P_E , where the value of f_{n_0} was the experimental zero load frequency rather than the theoretical value, were of a higher value than was anticipated from the theoretical calculation, as shown in Fig. 10 on p. 30. With the exception of the columns of L/p values of 166 and 137, the experimental values of the natural frequencies were lower than the calculated values at zero load. (See Table 3 on p. 31.) However, at an average load of 200 pounds the experimental values became larger than the calculated values and remained so for the rest of the loading cycle. Four experimental curves showed agreement with little scatter up to a P/P_E value of about 0.65. For values of P/P_E larger than 0.65 the amount of scatter increased and no general curve could be applied to the plotted values. One experimental curve, that of the seamless brass tube specimen, was considerably higher than the other curves, varying in values of $0.05 f_n/f_{n_0}$ at low P/P_E values to about $0.2 f_n/f_{n_0}$ at higher values of P/P_E .

TABLE 2
Experimental Values of f_n/f_{n_0} , P/P_E

Load	Spec I $L/\rho = 93$		Spec II $L/\rho = 107$		Spec III $L/\rho = 125$		Spec IV $L/\rho = 150$		Spec V $L/\rho = 166$		Spec VI $L/\rho = 187$		Spec VII $L/\rho = 137$	
	P/P_E	f_n/f_{n_0}	P/P_E	f_n/f_{n_0}	P/P_E	f_n/f_{n_0}	P/P_E	f_n/f_{n_0}	P/P_E	f_n/f_{n_0}	P/P_E	f_n/f_{n_0}	P/P_E	f_n/f_{n_0}
0	0.000	1.000	0.000	1.000	0.000	1.000	0.000	1.000	0.000	1.000	0.000	1.000	0.000	1.000
20													.118	.992
40													.236	.984
60													.354	.968
80													.472	.952
100	.010		.017		.031		.048	.989	.099	.977	.159	.971	.590	.937
120													.708	.906
140													.826	.875
160													.944	.844
200	.020	1.00	.034	0.991	.063	.991	.095	.978	.198	.955	.318	.942		
300	.030		.051		.094		.143	.966	.297	.934	.476	.870		
400	.040	1.010	.068	1.020	.126	.972	.190	.956	.396	.911	.635	.796		
500	.049		.084		.158		.238	.945	.495	.866	.794	.740		
600	.059	1.010	.101	1.025	.189	.954	.286	.934	.595	.800	.953	.652		
700	.069		.118		.220		.333	.923	.694	.744				
800	.079	1.010	.135	1.025	.252	.936	.381	.901	.793	.700				
900	.089		.152		.283		.428	.880	.892	.666				
1000	.099	1.010	.169	1.025	.314	.918	.476	.857						
1100	.109		.186		.346		.524	.835						
1200	.119	1.010	.203	1.025	.377	.900	.571	.814						
1300	.129		.220		.409		.619	.780						
1400	.139	1.005	.237	1.025	.440	.873	.666	.725						
1500	.149		.254		.472		.714	.704						
1600	.158	1.005	.271	1.025	.503	.845	.503	.660						
1700	.168		.287		.534		.809	.615						
1800	.178	1.000	.304	1.020	.566	.809								
1900	.188		.321		.597									
2000	.198	1.000	.338	1.020	.629	.781								
2100	.208		.355		.660									
2200	.218	1.000	.372	1.020	.692	.764								

NOTE: Specimens I-VI were of 17 St aluminum alloy round rod. Specimen VII was of seamless brass tubing having a 0.18 inch wall. All specimens were 23-3/8 inches long. For specimens I, II, and III the theoretical critical column load was used in calculating P/P_E .

THEORETICAL AND EXPERIMENTAL VALUES OF $\frac{F_n}{f_{n0}}$ VS $\frac{D}{D_0}$



SPEC.	$\frac{L}{D}$	SYMBOL
I	93	□
II	107	○
III	125	△
IV	150	○
V	166	△
VI	187	+
VII	137	x

EQUATION FOR THE THEORETICAL CURVE

$$F_n = \frac{\pi n^2}{2L} \sqrt{\frac{EI_0}{\rho A}} \sqrt{1 - \frac{D}{D_0}}$$

FIG. 10

TABLE 3

Theoretical Values of f_n Versus Load Compared to Experimental Values of f_n Versus Load

Load	Spec I $L/\rho = 93$		Spec II $L/\rho = 107$		Spec III $L/\rho = 125$		Spec IV $L/\rho = 150$		Spec V $L/\rho = 166$		Spec VI $L/\rho = 187$		Spec VII $L/\rho = 137$	
	f_{nT}	f_{nE}	f_{nT}	f_{nE}	f_{nT}	f_{nE}	f_{nT}	f_{nE}	f_{nT}	f_{nE}	f_{nT}	f_{nE}	f_{nT}	f_{nE}
0	150	120	131	116	112	110	93.5	91	84.1	90	74.8	69	62.5	64
20													58.7	64
40													54.6	63
60													50.3	62
80													45.4	61
100							91.2	90	79.8	88	68.6	67	40.0	60
120													33.8	58
140													26.1	56
160													14.8	54
200	148.6	120	128.8	114	108.4	109	89.0	89	75.2	86	61.8	65		
300							86.5	88	70.4	84	54.2	60		
400	147.0	121	126.6	118	104.8	107	84.1	87	65.2	82	45.2	55		
500							81.6	86	59.8	78	33.9	51		
600	145.6	121	124.2	120	101.0	105	79.1	85	53.5	72	16.25	45		
700							76.3	84	46.6	67				
800	144.0	121	121.8	120	97.0	103	73.5	82	38.3	63				
900							70.8	80	28.9	60				
1000	142.5	121	119.5	120	92.8	101	67.7	78						
1100							64.5	76						
1200	141.0	121	117.0	120	88.5	99	61.3	74						
1300							57.8	71						
1400	139.1	120.5	114.6	120	83.8	96	54.0	66						
1500							50.0	64						
1600	137.6	120.5	111.8	120	79	93	45.6	60						
1700							40.9	56						
1800	136.0	120	109.2	119	73.8	89								
1900														
2000	134.5	120	106.6	119	69.2	86								
2100														
2200	132.6	120	103.8	119	62.2	84								

NOTE: Specimens I-VI were of 17 ST aluminum alloy round rod. Specimen VII was of seamless brass tubing having a 0.18 inch wall. All specimens were 23-3/8 inches long.

The broad scatter of the experimental values beyond the P/P_E value of 0.65 can partially be attributed to the rapid damping out of the vibration caused by the closeness to the critical load which prevented accurate readings of the frequency introducing an approximate error of 5 cps. Another factor that appeared when the values were plotted could have been the machining done on the specimen ends. It was noticed that the specimens done by one machinist were in fairly close agreement to about 0.75 P/P_E but showed a variation with the specimens done by another machinist. The error introduced in this manner may have been caused by the method of forming the round at the extreme ends.

The deviation of the brass tubing specimen can probably be attributed to two factors. The main factor causing the higher values in the f_n/f_{n_0} ratio is that the specimen had a very low critical load and as previously found with the other specimens there was some difficulty in determining the frequencies when close to the buckling range. The other factor is the high damping capacity of brass, which also contributed to the difficulty in determining the frequencies.

The specimens that had the lowest slenderness ratios, 93 and 107, showed very little difference in natural

frequency under the loads applied. The tendency of the natural frequencies of these specimens was to increase a few cycles per second from zero load to a load of about 200 pounds. At that point the values leveled off throughout the loading range. It might be noted that these specimens were in the transition range from the short column range to the long column range.

In order to determine whether the presence of a lubricant on the ends of the specimens had any effect on the natural frequency, tests were made of specimens in an absolutely dry condition and then with lubrication. The lubricants used were mineral spirits and oil. The tests showed no apparent change at any increment of the load.

CHAPTER V

CONCLUSION

From the results shown by the experimentation, it appears that the often found discrepancy between a theoretical analysis and observations is present in this case. However, before making any statement to the effect that the theory involved in determining the variation of the natural frequencies of columns under load is of only general interest, it is the recommendation of the writer that more data be taken in a broader range of slenderness ratios that are included in the long column range.

There would undoubtedly be some variation between the actual and theoretical values of the natural frequencies due to the initial conditions set up in determining such values. It is almost an impossibility to experimentally equal the ideal conditions used in the theory. The most difficult condition to equal is that of loading. In the theory the load remains constant throughout the vibration by moving with the oscillating ends. In this experiment it was found that the inertia of the load applicator prevented such rapid movements. However, the change in the load was found to be very small.

Another factor that is involved is the problem of friction at the end supports and the internal friction of the specimens.

The fact that some damping was present in the experimentation¹ and that no damping was included in the theoretical analysis might provide an explanation for the higher experimental values of f_n/f_{n_0} . Timoshenko in the book Vibration Problems in Engineering,² briefly cited a reference³ which presented a differential equation for the lateral free vibration of long bars that included damping. The source of this reference was not available to the writer.

The theory seemed to be more at variance with the testing when specimens near the short column range were used. It would be well to investigate this range more fully and if possible determine some method of predicting the natural frequencies more accurately.

This investigation was carried out with several handicaps affecting the general results. The major

1. For a brief discussion of the types of damping present see Appendix A.

2. Timoshenko, op. cit., p. 332.

3. H. Holzer, Zeitschr. f. angew. Math. u. Mech. V. VIII, (1928), p. 272. See also K. Sezawa, Zeitschr. f. angew. Math. u. Mech., V. XII (1932), p. 275.

handicap was that of limitations imposed by the loading system used. The system used in this investigation was necessarily of a gas-fluid type. The load was applied by a ram that was operated by hydraulic fluid. Because of this a column of fluid was retained in the system to prevent any leakage losses in the fluid connections. The gas was used because of its low inertia and because it was the best available source of constant pressure. The use of a gas as the method of loading appears to be the best but it necessitates a gas operated ram. The method of changing the gas pressure was rather poor because of the type of release valve used. High pressure valves with a suitable reduction system would be of great advantage when operating at low loads.

In determining the frequencies of the specimens, the audio oscillator that was used was limited to a minimum frequency of 20 cps. Therefore, it was of little use when specimens of a L/ρ higher than 190 were tested. It was also necessary to make use of Lissajous figures when the natural frequencies were above 90 cps because of the narrow distance between calibrations above that frequency.

The test rig was of such a design that only specimens of one length could be used. This limited the usable values of L/ρ because of the machining that would have been required to have a large number of different

L/ρ values. With movable end supports, the number of different specimens could be increased greatly.

Due to the lack of material that could be used for specimens only two types were used. They were (1) solid round aluminum rod, and (2) seamless brass tubing. It is the opinion of the writer that specimens of cross sections common to aircraft structures should be tested because of their applicability to aircraft design.

The mechanical oscillator used in the resonance tests operated at a fixed frequency throughout a test. For this reason the number of tests was limited to those specimens whose frequencies under load closely approximated the frequency of the forced vibration. If a variable speed drive were used, the number of usable specimens would increase greatly. This would be an advantage in possible fatigue studies of columns, and is possibly a better method of determining the natural frequencies of columns at any load.

APPENDIX A

DAMPING: TYPES PRESENT AND EFFECTS

Because of the design of the testing rig, only two types of damping were present in the experimentation. They were: (1) Coulomb damping or damping due to friction, and (2) Solid damping or damping due to internal friction within the specimens themselves.

Coulomb damping was present at the end supports and increased with an increase in loading. This is in accordance with the equation of Coulomb damping $F = \mu N$ where F is the damping force, μ is the coefficient of friction and N is the normal force. This type of damping, however, has no effect on the frequency of vibration.¹

The presence of solid damping is self-explanatory. The degree of damping is proportional only to the displacement and is independent of the frequency of vibration.² The general equation for solid damping is $F = \gamma kx$ where the constant of proportionality is written in the terms of a non dimensional damping factor γ and the spring constant k . The damping factor γ is proportional

1. W. T. Thompson, Mechanical Vibrations, p. 57.
2. Ibid.

to the stress developed in the specimen.³ In this investigation the maximum stress attained in any one specimen was under 4000 PSI and in the range from 0 - 10,000 PSI the damping factor can be considered constant without appreciable error.

Since the decay of amplitude of free vibration is due to dissipation of energy it is of interest to determine the nature of the damping force and the energy dissipated by it.

Consider a general case of a harmonic damping force lagging the displacement by a phase angle ϕ . The displacement and force may then be represented by

$$x = X \sin pt$$

$$F = F_0 \sin (pt - \phi)$$

The work done by this force per cycle of motion then becomes

3. E. V. Potter, Damping Capacity of Metals, Report of Investigation 4194, Bureau of Mines, U. S. Department of Interior, March, 1948, p. 25.

$$\begin{aligned}
 W &= \int F dx = \int_0^{\frac{2\pi}{p}} F \frac{dx}{dt} dt \\
 &= p F_0 X \int_0^{\frac{2\pi}{p}} \cos pt \sin(pt - \phi) dt \\
 &= p F_0 X \left[\cos \phi \int_0^{\frac{2\pi}{p}} \sin pt \cos pt dt - \sin \phi \int_0^{\frac{2\pi}{p}} \cos^2 pt dt \right]
 \end{aligned}$$

The first integral is necessarily equal to zero and the second integral is equal to π/p . The work done per cycle then becomes equal to

$$W = -\pi F_0 X \sin \phi$$

where the negative work indicates a dissipation of energy.

It is evident from this equation that the maximum energy is dissipated when the phase angle ϕ is 90 degrees. Energy dissipation in harmonic motion is possible only by the component of force lagging the displacement by 90 degrees. Since such a force is opposite in phase to the velocity, it can be concluded that damping forces in harmonic motion must always be opposite in direction to the velocity.

In order that the effects of damping be included in this investigation, it is necessary to know what damping

forces are present. This necessitates an accurate measurement of the friction coefficient in Coulomb damping throughout the loading range and also an accurate measurement of the internal friction in the columns throughout the loading range. Obviously this would necessitate investigation into such coefficients which is beyond the scope of this paper.

APPENDIX B

A RESUME' OF INVESTIGATIONS OF VIBRATION IN AIRCRAFT

One of the most important problems in aircraft structural design is that of vibration. A customary method of design for vibratory load is to design the airframe to withstand the greatest load that can be expected. This method is probably satisfactory for erratically varying loads such as gust loads, but where periodic vibrations, such as set up by the engine, are present, the failure of various members has occurred.

In the case of the B-36 where the wing spars are extremely long the failure of these spars in operational flights has been apparently of the fatigue type. In the specific case of engine mounts failure has been definitely of the fatigue type.

Since the inception of powered flight many investigations concerning the failure of various elements of aircraft structures have been made. One of the first papers on vibrations or vibratory loads with respect to aircraft structures was published in England by W. L. Cowley and H. Levy¹ in 1919. The authors made a mathematical

1. W. L. Cowley and H. Levy, "Vibration and Strength of Struts and Continuous Beams Under End Thrusts," Proceedings of the Royal Society of London, XCV, Series A (July, 1919), 440-457.

analysis of the problem of vibration and strength of struts and continuous beams under end thrusts. In this analysis the authors considered continuous beams whose flexural rigidity varied from bay to bay and whose supports were in a state of periodic vibration. A very generalized equation of three moments was derived and the conditions for resonance and crippling were expressed by determinants. A general equation where the restrictions were removed in regard to the constancy of the end thrusts and of the flexural rigidity was applied to the particular case of a strut of variable flexural rigidity.

In 1925, C. F. Jenkins² conducted a series of fatigue studies on aircraft metals using the resonance method devised by Hopkinson in 1911. The test specimens were straight rods of approximately 0.10 inch in diameter and varying in lengths from 2.54 inches to 19.4 inches.

Hertal,³ in 1931, made an investigation to show how the strength of airplane parts can be tested with respect to dynamic stresses with and without superposed static

2. C. F. Jenkins, "High Frequency Fatigue Tests," Proceedings of the Royal Society of London, CIX, Series A (1925), 119.

3. H. Hertal, Dynamic Breaking Tests of Airplane Parts, NACA TM No. 968, 1933.

loading, and to what extent the dynamic strength of the parts depends on their structural design. The importance of local stress concentrations, due to abrupt changes in cross section, notches, holes, rivets, etc., was discussed. It was also stated that the results of endurance tests of the material in the form of test bars can be applied to the material actually incorporated in the structure only when the stresses in the structure, including local increments, are known.

In 1938, the Goodyear-Zeppelin Corporation⁴ made some fatigue studies in which the specimens were subjected to reversed axial loadings. This method consisted of the incorporation of one or two reciprocating motors in a resonance system of which the specimen acted as the spring element. In the same year, Bleakney⁵ conducted the same type of test on full-scale wing beams that contained various stress raisers. However, his work was not conclusive enough and shortly afterward Brueggman, Krupen, and Roop⁶ carried on this method of fatigue

4. Goodyear-Zeppelin Corporation, Preliminary Fatigue Studies of Aluminum Alloy Aircraft Girders, NACA TN No. 637, 1938.

5. Wm. N. Bleakney, Fatigue Testing of Wing Beams by the Resonance Method, NACA TN No. 660, 1938.

6. W. C. Brueggman, P. Krupen, and F. C. Roop, Axial Fatigue Tests of 10 Airplane Wing-Beam Specimens by the Resonance Method, NACA TN No. 959, 1944.

research by testing ten wing-beam specimens. Some of the specimens used in this research had been in flight service, while the rest were not. It was found that the specimens that had not been in service were stronger in fatigue than those that had, indicating that the used beams had been subjected to fatigue while in service. In addition to the wing-beam tests, axial fatigue tests were made on coupons machined from the flanges. These coupons contained stress raisers in the form of holes and idle rivets. The purpose of the investigation was to determine the effect, on the fatigue strength of a full-size structure, of several types of stress concentration and to determine whether it was practicable to design such a structure on the basis of test results obtained on relatively simple coupon specimens containing typical stress raisers. The investigation, however, failed to disclose a method of design.

Kaul,⁷ in 1941, presented a method of analysis of the time and fatigue strength of aircraft wing structures by making a statistical analysis of a large number of data covering the wing stressing of several aircraft. He

7. Hans W. Kaul, Statistical Analysis of the Time and Fatigue Strength of Aircraft Wing Structures, NACA TM No. 992, 1941.

claimed that it is possible by this method to estimate the probable number of times loads of a given magnitude will be applied to the wing structure over a period of flying time depending on the class of aircraft and to adjust the ground tests accordingly.

In 1939, S. Lubkin⁸ made a mathematical analysis of the stability of columns under periodically varying axial loads. In this investigation a constant axial load was applied to a column and a harmonically varying axial load was superposed on the constant load. It was shown that the frequency and amplitude of the harmonic load greatly affected the stability of the column. It was implied that it was nearly impossible to experimentally prove the analysis because of the fine limits of the varying load required to stay within the stable range. The problem was again presented in 1939 by J. J. Stoker and S. Lubkin.⁹ Nothing new was added to the original presentation. However, mention was made of a paper by Utida and Sezawa¹⁰

8. Samuel Lubkin, Stability of Columns Under Periodically Varying Loads. A bound thesis for Doctor of Philosophy degree, New York University, 1939.

9. J. J. Stoker and Samuel Lubkin, "Stability of Columns and Strings Under Periodically Varying Forces," Quarterly of Applied Mathematics, I, No. 3 (October, 1943), 215-236.

10. I. Utida and K. Sezawa, "Dynamical Stability of a Column Under Periodic Longitudinal Forces," Report of the Aero. Res. Inst., Tokyo Imp. Univ., XV (1940), 193.

who made an investigation, both experimentally and theoretically, into the dynamic stability of a column under periodic longitudinal forces. In the experiments, the columns were in a partially fixed position and the constant part of the load was equal to zero.

A method of dynamic research and several applications of this method was reported by Bernhard¹¹ in 1937. In this method, vibrations are induced by centrifugal forces resulting from rotating eccentric disks. This method is based on the principle of applying small periodic loads. Another investigation utilizing the application of periodic forces was made by the Aluminum Company of America and reported by Templin¹² in 1939. The investigation, starting in 1935, covered the fatigue testing of several types of structural specimens. Several types of fatigue testing machines were constructed and each was used for a specific type of specimen. The machines utilized electric motors of fixed frequencies, that actuated a lever system that applied a periodic force to the specimen.

11. Rudolph K. Bernhard, "Dynamic Tests by Means of Induced Vibrations," Proceedings of the American Society for Testing Materials, XXXVII, II (1937), 634.

12. R. L. Templin, "Fatigue Machines for Testing Structural Units," Proceedings of the American Society for Testing Materials, XXXIX (1939), 711.

In 1947, Findley¹³ presented a fatigue testing machine that permitted testing of specimens in axial tension or compression. The specimens used, however, were of the type used in rotating beam tests, i. e. small specimens.

In searching for reports on column testing many were found that dealt with the impact strength of columns. One of the latest reports is that by Hoppmann¹⁴ published in December 1949. This investigation was theoretical in nature with several numerical examples illustrating the theory.

13. W. N. Findley, "New Apparatus for Axial Load Fatigue Testing," ASTM Bulletin 147 (August 1947), 54.

14. W. H. Hoppmann, 2nd, "Impact of a Mass on a Column," Journal of Applied Mechanics, (December, 1949), 370-374.

BIBLIOGRAPHY

Books and Pamphlets:

- Bleakney, William M., Fatigue Testing of Wing-Beams by the Resonance Method, National Advisory Committee for Aeronautics, TN 660, Washington, D. C., 1938.
- Brueggman, W. C., Krupen, P., and Roop, F. C., Axial Fatigue Tests of 10 Airplane Wing-Beam Specimens by the Resonance Method, National Advisory Committee for Aeronautics, TN 959, Washington, D. C., 1944.
- Goodyear-Zeppelin Corporation, Preliminary Fatigue Studies on Aluminum Alloy Aircraft Girders, National Advisory Committee for Aeronautics, TN 637, Washington, D. C., 1938.
- Hertal, Heinrich, Dynamic Breaking Tests of Airplane Parts, National Advisory Committee for Aeronautics, TM 698, Washington, D. C., 1933.
- Kaul, Hans W., Statistical Analysis of the Time and Fatigue Strength of Aircraft Wind Structures, National Advisory Committee for Aeronautics, TM 992, Washington, D. C., 1941.
- Potter, E. V., Damping Capacity of Metals, Bureau of Mines, U. S. Department of Interior, R.I. 4194, Washington, D. C., March 1948.
- Thompson, William T., Mechanical Vibrations. Prentice-Hall, Inc., New York, 1948.
- Timoshenko, S., Vibration Problems in Engineering (2nd ed.). D. Van Nostrand Company, Inc., New York, 1937.

Articles:

- Bernhard, Rudolph K., "Dynamic Tests by Means of Induced Vibrations," Proceedings of the American Society for Testing Materials, XXXVII, II (1937), 634-638.
- Cowley, W. L. and Levy, H., "Vibration and Strength of Struts and Continuous Beams Under End Thrusts," Proceedings of the Royal Society of London, XCV, Series A (July, 1919), 440-457.
- Findley, W. N., "New Apparatus for Axial-Load Fatigue Testing," American Society for Testing Materials Bulletin, CXLVII (August, 1947), 54.
- Hoppmann, W. H., 2nd., "Impact of a Mass on a Column," Journal of Applied Mechanics, (December, 1949), 370-374.
- Jenkins, C. F., "High Frequency Fatigue Tests," Proceedings of the Royal Society of London, CIX, Series A (1925), 119.
- Stoker, J. J. and Lubkin, S., "Stability of Columns and Strings Under Periodically Varying Forces," Quarterly of Applied Mathematics, I (October, 1943), 215-236.
- Templin, R. L., "Fatigue Machines for Testing Structural Units," Proceedings of the American Society for Testing Materials, XXXIX (1939), 711.

Manuscripts:

- Lubkin, Samuel, Stability of Columns Under Periodically Varying Load. A bound thesis for Doctor of Philosophy Degree, New York University, 1939.